
Robust Flow-based Conformal Inference (FCI) with Statistical Guarantee

Youhui Ye

Department of Statistics
Virginia Tech, USA
yye1997@vt.edu

Meimei Liu

Department of Statistics
Virginia Tech, USA
meimeiliu@vt.edu

Xin Xing

Department of Statistics
Virginia Tech, USA
xinxing@vt.edu

Abstract

Conformal prediction aims to determine precise levels of confidence in predictions for new objects using past experience. However, the commonly used exchangeable assumptions between the training data and testing data limit its usage in dealing with contaminated testing sets. In this paper, we develop a series of conformal inference methods, including building predictive sets and inferring outliers for complex and high-dimensional data. We leverage ideas from adversarial flow to transfer the input data to a random vector with known distributions, which enable us to construct a non-conformity score for uncertainty quantification. We can further learn the distribution of input data in each class directly through the learned transformation. Therefore, our approach is applicable and more robust when the test data is contaminated. We evaluate our method, robust flow-based conformal inference, on benchmark datasets. We find that it produces effective prediction sets and accurate outlier detection and is more powerful relative to competing approaches.

1 Introduction

Deep learning algorithms are increasingly being applied in modern decision-making processes. For example, self-driving cars detect objects using complex data from cameras and other sensors [Rao and Frtunikj, 2018]. Intelligent disease diagnosis use data from various types of medical imaging to clinical records [Bakator and Radosav, 2018]. In such cases, the test data usually contains noisy or contaminated observations or has outliers that have not been seen in limited training data. It is crucial to develop robust methods to quantify the uncertainty of their predictions in the decision-making process.

Conformal prediction constructs valid prediction intervals instead of point estimates for new objects using past data. It was introduced by Vovk et al. [2005], Vovk [2012], and has a wide application in regression [Lei and Wasserman, 2014], classification [Romano et al., 2020]. The classical conformal prediction uses scores outputted by black-box classifiers such as deep neural networks to build the confidence sets. However, the probabilities output by convolutional neural networks (CNNs) is overconfidence or underconfidence, which is observed as the probability values concentrated to 0 or 1 [Nixon et al., 2019], leading to inaccurate conformal prediction. In order to calibrate the probabilities, data-splitting is one commonly used strategy to estimate the distribution of input data [Romano et al.,

2020, Angelopoulos et al., 2020]. It uses the first half of the data to train the model and uses the second half of the data to evaluate the distribution, which inevitably causes the power loss.

In this paper, we develop a flow-based conformal inference (FCI) to construct prediction intervals for target labels with statistical guarantee. A notable feature of FCI is its ability in learning the distribution of the complex training data for each class. To achieve this feature, we focus on learning a pair of transformations between the input data (viewed as the real domain) and its latent domain via the adversarial generative model [Goodfellow et al., 2014b]. By adding the cycle consistency constrain [Zhu et al., 2017], the transformation can reserve the conditional distribution of our complex input data given each class label. Furthermore, the latent domain contains variables satisfying the exchangeable condition, which is guaranteed by the symmetric design of the neural network architecture. Then, to develop the predictive region, we consider testing whether a prediction is from a given class. Leveraging on the learned latent domain, we construct test statistics with an asymptotic Gaussian distribution, and derive a valid p -value that enjoys the controlled type-I error rate. We also show that the proposed p -value can serve as a basis for various inference tasks, including building predictive sets and outlier detection.

We further consider the cases where the outliers are presenting in the test data. For example, in diagnosis, the patient in testing set may has a rare disease that deviate from the training data. It is harmful to give a wrong predictive set including other types of disease or healthy. Instead, detecting it as a outlier for doctor’s further review is a better decision. However, classical conformal predictions are prone to be unstable in such cases since the commonly used assumption that the training and test data are exchangeable [Gibbs and Candes, 2021] is not valid when presenting outliers in test data. We remark that, learning the distribution of the complex data is an inherent property of FCI. Therefore, we can formulate the outlier detection through the corresponding test statistics characterization. Depending on the distinguishability of the test statistics, a sensitivity test can detect the outliers which deviation from the null distribution [Xing et al., 2019].

Related Work

In classical approaches, Bayesian neural networks [Neal, 2012] and bootstrap methods [Gupta et al., 2022] are used to quantify uncertainty. These approaches do not scale well on large data sets due to the computational bottleneck in the sampling process. Recently, conformal prediction is an approach for generating predictive sets that satisfy the coverage property. The most popular approach in this line is a data-splitting version known as the split conformal prediction that enables conformal prediction methods to be deployed for any classifier [Papadopoulos et al., 2002, Lei and Wasserman, 2014, Angelopoulos et al., 2020]. This line of work assumes the test data and training data are exchangeable, which limits its application when there are outliers or distributional shifts in the test data. Gibbs and Candes [2021] introduce a tunable parameter for adaptive data-splitting methods to deal with the distributional change. However, it is still challenging to handle cases where outliers appear.

The probability distribution is an essential tool to quantify the uncertainty in various modern inference tasks. Compared with classical statistical methods such as Bayesian inference [Meng, 1994], nonparametric density estimation [Davis et al., 2011] and bootstrap [Stine, 1985], flow-based generative models leverage the ability to learn the distribution in complex data in a scalable fashion. Normalizing flows represent learning an invertible transformation from input data to a latent variable with a known density. To achieve this, the neural density estimators have to impose heavy constraints. To mitigate this issue, Liu et al. [2021] employ the cycle-consistency constraint in cycleGAN [Zhu et al., 2017], to learn a pair of transformations between the latent variable space and the data space, which demonstrates state-of-the-art performance in various applications. Motivated by the power of the flow-based method in learning complex distribution, we propose a conditional adversarial flow network as a basis for our conformal inference framework.

2 Method

Uncertainty quantification (UQ) has been studied extensively in both the fields of statistics and machine learning. We first consider the fundamental statistical problem for testing whether an observation X_{new} belongs to the l th class for $l \in \{1, \dots, L\}$. Let F_l be the distribution of X_{new} given $Y_{\text{new}} = l$. We consider the following hypothesis

$$H_0 : X_{\text{new}} \sim F_l \quad \text{v.s.} \quad H_1 : X_{\text{new}} \not\sim F_l. \quad (1)$$

This hypothesis testing problem serves as a basis for performing various of inference tasks such as building conformal predictive sets and detecting outliers. The major quantity for UQ is the p -value for (1), which is the probability of obtaining test result at least as extreme as the result observed. We define $\alpha \in (0, 1)$ as the predefined type-I error which also known as the “false positive” rate and $\pi_l(X_{\text{new}})$ as the the p -value for hypothesis testing (1) such that

$$P(\pi_l(X_{\text{new}}) \leq \alpha | Y_i = l) \leq \alpha \quad (2)$$

i.e., the p -value is uniformly distributed in $(0, 1)$. For example, suppose X_i is one-dimensional following known Gaussian distribution with mean μ_l and variance σ_l^2 conditioned on $Y_i = l$. We then have the explicit form of p -value, i.e., $\pi_l(X_i) = 2(1 - \Phi(X_i))$ where Φ is the CDF. In this case, the univariate Gaussian distribution has a light tail, which makes p -value decreases exponentially for a value far from the mean and thus tends to have a high power to detect the extreme values. With p -values known, we can construct the predictive set for X_{new} as

$$C(X_{\text{new}}) = \{l : \pi_l(X_{\text{new}}) \geq \alpha\}.$$

However, the real applications usually have high-dimension covariates, which is challenging to estimate the conditional distribution F_l and to find a function of X_i as a valid p -value satisfying (2). Recently, the development of adversarial generative models [Zhu et al., 2017] enables the power to learn the distribution of complex data. Without loss of generality, denote $X \in \mathcal{X}$, and $Z \in \mathcal{Z} \subset \mathbb{R}^d$ as a random variable with known distribution. We design a bidirectional conditional generative neural network for learning an invertible transformation $G_l : \mathcal{X} \rightarrow \mathcal{Z}$ such that the conditional density of X can be expressed as

$$f_l(x) = f_z(z) |\det(J_z)|^{-1} \quad (3)$$

where $J_z = (\partial G_l^{-1}(z) / \partial Z^\top)$ is the Jacobian matrix of G_l^{-1} at z . In this section, we first introduce a conditional adversarial flow to learn G_l while maximizing the power in classification tasks. Based on the learned transformation, we propose a novel p -value for hypothesis problem in (1) which serves as a basis for our conformal inference framework.

2.1 Conditional Adversarial Flow

Conditional on $Y = l$, our following task is to learn the conditional distribution of X via the mutually inverse mappings $G_l : \mathcal{X} \rightarrow \mathcal{Z}$ and $I_l = G_l^{-1} : \mathcal{Z} \rightarrow \mathcal{X}$. Zhu et al. [2017] introduced cycle consistent adversarial networks for unpaired image translation tasks. We employ the cycle consistency loss to transfer the input data X to Z , where the latter random variable Z has a known distribution. Therefore, we can learn the distribution of X based on (3) and quantify the uncertainty in the complex sample space such as images. Intuitively, we can use deep adversarial generative networks to model the mappings G_l and I_l . In this paper, we focus on the image data using CNN structures; however, the framework can be generalized to model other data types by adjusting the neural network architecture.

Generative model for data (learning $G_l(\cdot)$) We propose to construct our generator based on a series of transposed convolutional filters Dumoulin and Visin [2016]. We consider Z from standard multivariate Gaussian distribution with density function $p_Z(z)$ defined as

$$p_Z(z) = (\sqrt{2\pi})^{-d} \exp\left(-\frac{\|z\|_2^2}{2}\right),$$

where $\|\cdot\|_2$ is the L^2 norm, and d is the dimension of Z . The generator G_l can be represented as

$$G_l = C^{(K)} \circ \dots \circ C^{(1)}(Z),$$

where $C^{(k)} = (C_1^{(k)}, \dots, C_{q_k}^{(k)})$ denotes the transposed convolutional layer with depth q_k . For example, the first transposed convolutional layer $C^{(1)}(Z)$ is based on each element of the vector Z . Then the output of the first transposed convolutional layer is

$$C_t^{(1)} = \sigma(\omega_{1t} \odot Z) \quad \text{for } t = 1, \dots, q_k,$$

where $C^{(1)}$ denotes the result of a transposed convolution, \odot denotes the transposed convolution operation, ω_{1t} is the t th filter in layer 1, and $\sigma(\cdot)$ is the activation function. In order to achieve the size of the target image X , we sequentially apply the transposed convolutional filters

$$C_t^{(k+1)} = \sigma(\omega_{k+1,t} \odot C^{(k)})$$

until the output dimension is equal to the image dimensions, and we denote the output as $C^{(K)}$. Then we propose the discriminator network $D_{G_l} : \mathcal{X} \rightarrow \{0, 1\}$, which attempts to determine if the generated image is real or fake. The output is the probability that X comes from the real data rather than the generated data. As shown in [Goodfellow et al., 2014a], the generator aims to maximize the failure rate of the discriminator, while the discriminator aims to minimize it. The two networks are locked in a two-player minimax game defined by the value function

$$V_{G_l}(G_l, D_{G_l}) = \min_{G_l} \max_{D_{G_l}} \mathbb{E}_{X \sim F_l} [\log D_{G_l}(\mathbf{Z})] + \mathbb{E}_{\mathbf{Z} \sim p_{\mathbf{Z}}} (\log(1 - D_{G_l}(G_l(\mathbf{Z}))). \quad (4)$$

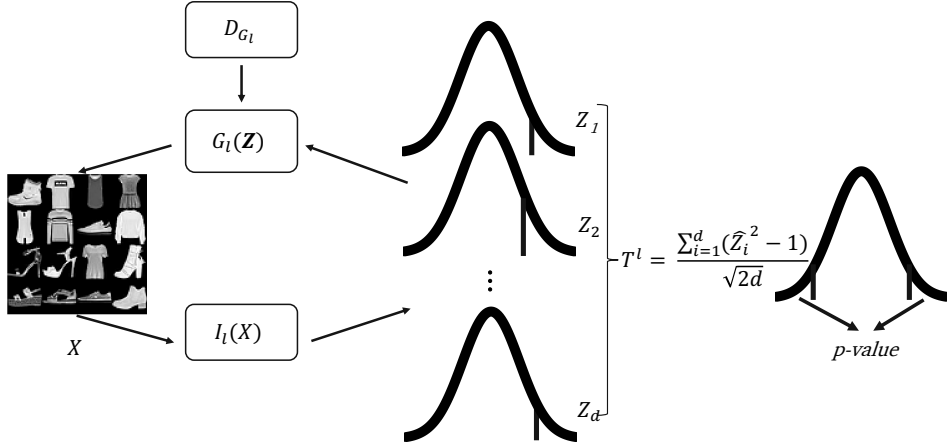


Figure 1: Illustration of flow-based conformal inference for image data. Z_1, Z_2, \dots, Z_d follow multivariate Gaussian distribution with mean zero and identity covariance matrix. T^l is our proposed non-conformity score constructed by latent representation $\hat{Z} = I(X)$. We construct two-sided p -value for hypothesis testing problem in (1) based on the distribution of T^l .

Inverse generative model (learning $I_l(\cdot)$) As shown in Figure 1, in order to estimate the conditional distribution F_l , we need to learn the inverse generator for transforming the data back into Euclidean space. We consider the base distribution of \mathbf{Z} is multivariate Gaussian with an identity covariance matrix since we aim to minimize the dependency among the entries in \mathbf{Z} . This construction will benefit us to have a valid asymptotic distribution.

Instead of using the discriminator, we consider using a distance measure \mathcal{M} . The maximum mean discrepancy (MMD) proposed by [Gretton et al., 2012] is a popular and suitable tool. Suppose there are two known probability measures μ and ν on latent space \mathcal{Z} . Given U and U' independent variables with probability measure μ , and V and V' independent variables with probability measure ν , the squared MMD is

$$\mathcal{M}^2[\mathcal{F}, \mu, \nu] = \mathbb{E}_{U, U'}[k(U, U')] - 2\mathbb{E}_{U, V}[k(U, V)] + \mathbb{E}_{V, V'}[k(V, V')]$$

where \mathcal{F} is a unit ball in a universal reproducing kernel Hilbert space \mathcal{H} defined on the compact set \mathcal{Z} . And $k(\cdot, \cdot) : \mathcal{Z} \times \mathcal{Z} \rightarrow \mathbb{R}$ is the corresponding reproducing kernel. [Gretton et al., 2012] also provides an unbiased sample estimate for observations U_i for $i = 1, 2, \dots, m$ and V_j for $j = 1, 2, \dots, n$ as

$$\mathcal{M}_u^2[\mathcal{F}, U_i, V_j] = \frac{1}{m(m-1)} \sum_{i=1}^m \sum_{j \neq i}^m k(U_i, U_j) + \frac{1}{n(n-1)} \sum_{i=1}^n \sum_{j \neq i}^n k(V_i, V_j) - \frac{2}{mn} \sum_{i=1}^m \sum_{j=1}^n k(U_i, V_j)$$

where the commonly used kernels are Gaussian, Laplacian, and energy kernels. We use the Gaussian kernel in our implementation.

It is worth noting that we eliminate the discriminator part for the inverse generator. That is simply because the deterministic discriminator is unable to tell whether the outputted vector is from a certain distribution. We directly use the MMD as a criterion to help the inverse generator produce high-quality samples that mimic the Gaussian distribution. The value function for learning I_l is defined as

$$V_I(I_l) = \min_{I_l} \mathbb{E}_{X \sim F_l, \mathbf{Z} \sim p_{\mathbf{Z}}} [\mathcal{M}_u(I_l(X), \mathbf{Z})].$$

As demonstrated in Zhu et al. [2017], it is necessary to supplement a cycle consistency loss, which can guarantee $X_i \in \mathcal{X}$ to be mapped to a desired output $\mathbf{Z}_i \in \mathbb{R}^d$, and vice versa. It essentially means $x \rightarrow G_l(x) \rightarrow I_l(G_l(x)) \approx x$, and $\mathbf{z} \rightarrow I_l(\mathbf{z}) \rightarrow G_l(I_l(\mathbf{z})) \approx \mathbf{z}$. We formulate the loss function as

$$V_{\text{cycle}}(G_l, I_l) = \min_{G_l, I_l} \{ \mathbb{E}_{X \sim F_l} [\|X - I_l(G_l(X))\|] + \mathbb{E}_{\mathbf{Z} \sim p_{\mathbf{Z}}} [\|\mathbf{Z} - G_l(I_l(\mathbf{Z}))\|] \}.$$

As shown in Figure 1, we combine the three networks into a cycle. The total loss consists of three parts as

$$V_{\text{total}}(G_l, D_{G_l}, I_l) = V_G(G_l, D_{G_l}) + V_I(I_l) + V_{\text{cycle}}(G_l, I_l)$$

which ensures us to have realistic images, distributions, and a one-to-one mapping, respectively.

2.2 Construct p -value and asymptotic property

Construct the non-conformity score function Using the cycled adversarial generative framework, we expect the inverse generator can construct a one-to-one mapping between input data and the target d -dimensional distribution. However, a d -dimensional statistic may not serve satisfactorily as a non-conformity score since it is hard to compare values in multi-dimensional space. Thus, we apply the "sum-of-square" function to \mathbf{Z} inspired by the Chi-squared test statistic. Let $\hat{\mathbf{Z}} = (\hat{Z}_1, \hat{Z}_2, \dots, \hat{Z}_d)^\top$ denote the output vector from inverse generator I_l . For simplicity, we omit the superscript l for \mathbf{Z} since the derivation is the same for any $l = 1, \dots, L$. We define the non-conformity score function as

$$T^l(X) = \sum_{i=1}^d \frac{\hat{Z}_i^2 - 1}{\sqrt{2d}}. \quad (5)$$

For a new observation X_{new} , we call $T_{\text{new}}^l = T^l(X_{\text{new}})$ as its non-conformity score for l th class. And it will play a major role in our inference and prediction methods.

In order to derive the asymptotic distribution of T_{new}^l , we introduce the following proposition to show the exchangeability of \hat{Z}_i . In the theoretical derivation, we consider the modern high-dimensional setting where the dimension of both X and \mathbf{Z} goes to infinity as n goes to infinity.

Proposition 1. *(Exchangeability) The distribution of the output of generator G is exchangeable, i.e.,*

$$(\hat{Z}_1, \hat{Z}_2, \dots, \hat{Z}_d) \stackrel{d}{=} (\hat{Z}_{\sigma(1)}, \dots, \hat{Z}_{\sigma(d)})$$

where $\sigma(1), \dots, \sigma(d)$ is a permutation of $1, \dots, d$.

The exchangeability of components of \mathbf{Z} in Proposition 1 arises due to the nature of the output operations in neural networks. Hidden nodes are fully exchangeable as the previous layer are added together to obtain the output. As this is a label switching problem, this gives way to a factorially growing number of equivalent modes as the number of hidden nodes and hidden layers increases. Next, we derive the asymptotic distribution of T based on the central limit theorem for the exchangeable triangular array in [Weber, 1980].

Theorem 1. (Asymptotic distribution) *Let $\hat{\mathbf{Z}}$ be the output of $I(\cdot)$, we assume that $KL(\hat{\mathbf{Z}} || \mathbf{Z}) = o(d^{-1})$. Then we have (1). $\mathbb{E}((\hat{Z}_1^2 - 1)(\hat{Z}_2^2 - 1)/2) \rightarrow 0$, (2). $\max_{1 \leq i \leq d} \frac{|\hat{Z}_i^2 - 1|}{\sqrt{2d}} \xrightarrow{P} 0$, (3). $\frac{1}{d} \sum_{i=1}^d \frac{(\hat{Z}_i^2 - 1)^2}{2} \xrightarrow{P} 1$ as $d \rightarrow \infty$. Then*

$$T^l(X) = \sum_{i=1}^d \frac{\hat{Z}_i^2 - 1}{\sqrt{2d}} \xrightarrow{D} \mathcal{N}(0, 1), \quad d \rightarrow \infty, \quad l = 1, \dots, L$$

where \xrightarrow{D} and \xrightarrow{P} denotes the convergence in distribution and probability, respectively.

The proof is included in the supplementary. Theorem 1 shows that our proposed non-conformity score converges to a standard Gaussian distribution which guarantees the inlier concentrating to the mean and the extreme value is on the exponential decay tail. Note that we assume the convergence rate is faster than $1/d$ which is a mild assumption since n is usually much larger than d in many

modern applications. The nice symmetric bell shape of standard Gaussian density function suggests us to define a two-sided p -value. Practically, based on n training data points, we define the p -value as

$$\pi_{\text{new}}^l = \pi^l(X_{\text{new}}) = 2 \min \left(\frac{|\{T_i^l : T_{\text{new}}^l \geq T_i^l\}|}{|A_l|}, \frac{|\{T_i^l : T_{\text{new}}^l \leq T_i^l\}|}{|A_l|} \right) \quad (6)$$

where $A_l = \{T_i^l = T^l(X_i) : Y_i = l\}$ and $|\cdot|$ denotes the cardinality operation here.

Corollary 1. *Assume that $KL(\hat{\mathbf{Z}} || \mathbf{Z}) = o(d^{-1})$. we have*

$$P(\pi_i^l \leq \alpha | Y_i = l) \leq \alpha.$$

as $n \rightarrow \infty$.

Corollary 1 shows that our proposed p -value can control the type-I error of the hypothesis.

Next, we design an additional layer to maximize the power of the test, i.e., we aim to refine the latent representation such that the conformal score can be used to distinguish the classes in the training data. Using the Bayes posterior probability, we have

$$P_i^l = P(Y_i = l | X_i) = \frac{P(X_i | Y_i = l)P(Y_i = l)}{\sum_{l=1}^L P(X_i | Y_i = l)P(Y_i = l)}. \quad (7)$$

For each conditional probability $P(X_i | Y_i = l)$, we transferred to the domain \mathcal{Z} using the mapping G_l . By density transformation in (3), we have

$$P(Y_i = l | X_i) = \frac{P(T_i^l | Y_i = l)P(Y_i = l)|\det(J_z^l)| |\det(J_T)|}{\sum_{l=1}^L P(T_i^l | Y_i = l)P(Y_i = l)|\det(J_z^l)| |\det(J_T)|}.$$

To increase the power, we consider the following loss function to increase the distinguishability of the T^l , i.e.,

$$L_l^{\text{pred}} = \mathbb{E}_{X \sim F_l} [\log P(Y = l | X)] + \mathbb{E}_{X \not\sim F_l} [\log(1 - P(Y = l | X))]$$

where L_l^{pred} is the cross entropy loss to ensure the nonconformity score T_l can distinguish l th class with others.

2.3 Implementation

Our construction of I_l and G_l are based on the popular neural network architecture including VGG Simonyan and Zisserman [2014] and Resnet He et al. [2016]. Particularly, we replace the output layer of I_l with a conformal layer and parallel apply the stochastic gradient algorithm for subsets of data. Take $l = 1$ as an example, $I_1(X_i)$ is trained to be as close to multivariate Gaussian distribution as possible for $\{X_i : Y_i = 1\}$, while $I_1(X_i)$ is trained to yield a relatively large T_i^1 for $\{X_i : Y_i \neq 1\}$. Though we train L neural networks, the computational cost is similar to the classification model since we sample size is smaller for each class. This will increase the power without changing the size of the test. We summarize the our implementation in Algorithm 1.

3 Conformal Inference for Classification

As introduced in the second and third chapters [Vovk et al., 2005], a higher non-conformity score indicates more difference between X_i and the sample of label y . [Papadopoulos, 2008] formulated the framework of applying inductive conformal prediction to neural networks (NN), where he used NN as the underlying algorithm to produce a non-conformity score. However, the classical conformal inference can only distinguish classes within the training labels. If outliers appear in the test data, the coverage probability of the constructed predictive set can not be controlled. In this section, we consider a more general case allowing outliers in the test data. Our inference tasks will be separated into two parts: one is to construct a predictive set for inliers, i.e., test data points with labels observed in training; the other one is to detect the outliers, i.e., test data points with unseen labels.

Algorithm 1 Flow-based Conformal Inference

Input: Test size α , training data set: $\{X_i\}_{i=1}^n$, training data set labels: $\{Y_i\}_{i=1}^n$, testing data set: $\{X_i\}_{i=n+1}^{n+m}$, number of epochs N .

- 1: **for** $l = 1, \dots, L$ **do**
- 2: Initialize G_l , D_{G_l} and I_l .
- 3: **for** epoch $= 1, \dots, N$ **do**
- 4: Train G_l , D_{G_l} and I_l simultaneously on $\{X_i : Y_i = l, i = 1, \dots, n\}$ to minimize $V_{\text{total}} = V_G + V_l + V_{\text{cycle}}$.
- 5: Train I_l on $\{X_i : Y_i \neq l, i = 1, \dots, n\}$ to minimize L_l^{pred} .
- 6: **end for**
- 7: Apply $T^l(X)$ to $\{X_i : Y_i = l, i = 1, \dots, n\}$ to obtain A_l .
- 8: **end for**
- 9: **for** $i = n + 1, \dots, n + m$ **do**
- 10: Based on non-conformity score pool A_l , we compute p -values $\boldsymbol{\pi}_i = \{\pi_i^1, \pi_i^2, \dots, \pi_i^L\}$.
- 11: Obtain posterior probabilities define in 7, i.e., $\mathbf{P}_i = \{P_i^1, P_i^2, \dots, P_i^L\}$.
- 12: **end for**

Output: Conduct statistical inference based on $\{\mathbf{P}_i\}_{i=n+1}^{n+m}$.

3.1 Predictive Set

We use the p -value outputted by Algorithm 1 as our UQ measure in classical statistical sense, i.e., a smaller p -value indicate stronger evidence to reject the hypothesis in (1). Then, we can output a prediction set

$$C(X_{\text{new}}) = \{l : \pi_{\text{new}}^l \geq \alpha\} \quad (8)$$

which satisfies for any predefined error rate $\alpha \in (0, 1)$. For the prediction task, it is usually hard to show the convergence of accuracy to the best of our knowledge. However, there are a lot of work ([Vovk et al., 2005], [Papadopoulos, 2008]) on the coverage probability coverage in literature. We mainly focus on this task, and show its coverage probability now.

Theorem 2. (*FCI predictive set coverage guarantee*). *If $Y_{\text{new}} \in 1, \dots, l$, we assume that $KL(\hat{Z}||Z) = o(d^{-1})$. Then for the predictive set defined in (8)*

$$P(Y_{\text{new}} \in C(X_{\text{new}})) \geq 1 - \alpha$$

as $n \rightarrow \infty$.

Theorem 2 shows that FCI can achieve pre-specified coverage probability. It is different from making direct use of softmax output of CNNs because it produces “real” probability.

Algorithm 2 FCI for predictive set

Input: Test size α , $\{\mathbf{P}_i\}_{i=n+1}^{n+m}$ from Algorithm 1.

- 1: **for** $i = n + 1, \dots, n + m$ **do**
- 2: Construct predictive set for i th sample $C(X_i) = \{l : \pi_i^l \geq \alpha\}$.
- 3: **end for**

Conduct statistical inference based on $\{C(X_i)\}_{i=n+1}^{n+m}$.

3.2 Outlier Detection

The outlier detection can be treated as an unsupervised since the labels of outliers are not available during the training. The flow-based model described above can adapted into this scenarios since we learned all the conditional distribution in each classes in the training. If all the hypothesis in 1 for $l = 1, \dots, L$ has been rejected, it means the points is extreme for all the training classes. Then we conclude that the new data point is an outlier and use our p -values to control the type-I error rate, i.e., the rate of false detection of outliers.

Corollary 2. (*Type I error of FCI outlier detection*). *If $Y_{\text{new}} \in \{1, \dots, L\}$, then we have (8)*

$$P(C(X_{\text{new}}) = \emptyset | Y_i \in \{1, \dots, L\}) \leq \alpha$$

as $n \rightarrow \infty$ for the predictive set defined in 8.

Corollary 2 can be proved in the same way as Theorem 2. It states that an inlier will be mistakenly classified as an outlier of the probability at most α . It is verified in our experiment 2.

4 Numerical Results

As far as we know, the first attempt to construct a predictive set should be including classes from highest to lowest probability (see [Platt et al., 1999, Guo et al., 2017]) until their sum exceeds $1 - \alpha$. A brief illustration of the method would be: if we have s_1, s_2, \dots, s_L as the softmax output of a CNN, we get them ordered first, producing $s_{(L)}, s_{(L-1)}, \dots, s_{(1)}$ and the corresponding indexes i_1, i_2, \dots, i_L . The predictive set $C(X_i)$ is $\{i_1, i_2, \dots, i_c\}$ if $\sum_{l=1}^{c-1} s_{(L-l+1)} < \alpha$ and $\sum_{l=1}^c s_{(L-l+1)} \geq \alpha$. Among numerous improvements to Naive, we choose to compare with [Romano et al., 2020]’ method. We also compare our approach with the data-splitting conformal predictive method in [Romano et al., 2020], as Adaptive Prediction Sets (APS). Their work can be applied to any black-box algorithm with a split-conformal calibration. In experiment 1, we compare different methods under the regular setting without outliers. In experiment 2, we test our model performance under different contamination rates, i.e., with outliers in varying percentages. Our experiments are based on the benchmark data set Fashion-MNIST (<https://github.com/zalandoresearch/fashion-mnist>). There are ten classes in total, each of which has 6000 samples for in training data set and 1000 samples in the testing data set.

4.1 Experiment 1: Fashion-MNIST data

Experiment settings We consider two popular neural network architecture ((VGG16, ResNet18)) to implement Naive, APS and our FCI approach. We used Adam optimizer in all experiment settings. In all settings, we set the size α to be 0.05. We compared the performance of three methods mainly on two criteria: coverage and size.

$$\text{coverage} = \frac{\sum_{i=n+1}^{n+m} I_{\{i: Y_i \in C(X_i)\}}}{m}, \text{ and size} = \frac{\sum_{i=n+1}^{n+m} |C(X_i)|}{m}$$

Meanwhile, we reported the Top-1 and Top-3 accuracy to give a general estimate of the quality of CNNs for Naive and APS methods.

Model	Accuracy			Coverage			Size		
	Top-1	Top-3	Naive	APS	FCI	Naive	APS	FCI	
VGG16	0.8877	0.9827	0.8806	0.9458	0.9489	1.0739	1.3709	1.1523	
ResNet18	0.8898	0.9836	0.8983	0.9468	0.9526	1.1426	1.3436	1.2672	

Table 1: **Results on Fashion-MNIST** We report the coverage and size of optimal Naive, APS, FCI sets. Top-1 and top-3 accuracies are also recorded (Same for Naive and APS). Each result is the mean of 100 independent trials.

Both VGG16 and ResNet18 have around 89% prediction accuracy on Fashion-MNIST. Naive failed to achieve desired coverage probability. However, APS achieved 95% coverage probability in both cases. And the average size of prediction sets increased around 28% and 18% accordingly. FCI also covers the true class labels at around 95% times, but the average size of prediction sets increased only 7% and 11% compared to Naive. Our proposed method FCI can perform equally well on coverage but have a smaller size than APS. It partially illustrates the advantage of FCI: it preserves more information from the sample space \mathcal{X} .

In addition, we numerically verify the distribution of our proposed p -value is uniform in $(0, 1)$. Figure 2 shows the histograms of π_i^l under the null hypothesis, i.e., $\{\pi_i^l : Y_i = l\}$. For most of them, we see the p -values distribute uniformly, and the type-I error rates are around 5% for all classes. It demonstrates the FCI’s ability to measure the randomness in the sample space \mathcal{X} and avoid the problem of overconfidence or underconfidence in classical CNN output.

4.2 Experiment 2: Fashion-MNIST data with outliers

Since Naive and FCI do not have the capacity for outlier detection, we only ran this experiment for FCI. All experiment settings do not change except that the 10th class, *Ankle boot*, was removed from the training data set. So the training data sample size is 54000. We set contamination rate γ , which denotes the ratio of outlier sample size and inlier sample size. We consider two cases with 3% and

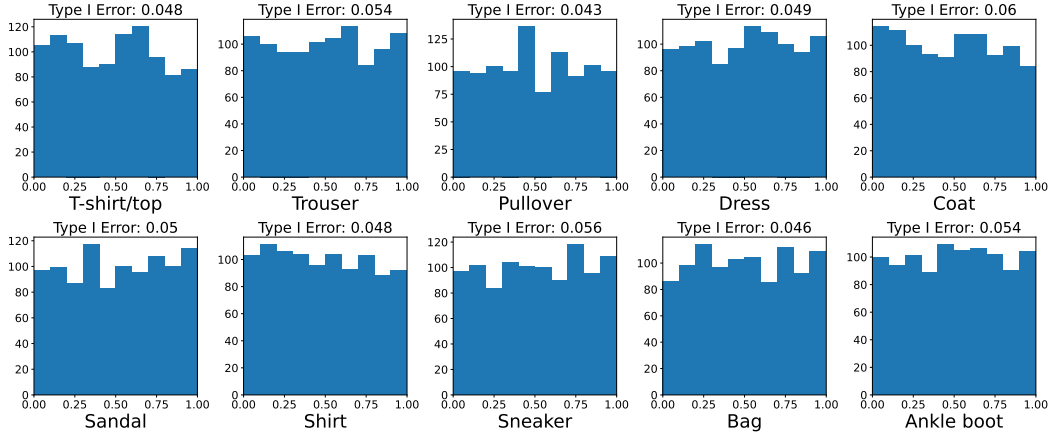


Figure 2: The histograms of $\{\pi_i^l : Y_i = l\}$ for $l = 1, \dots, 10$. They are expected to have uniform distributions.

6% outliers. For inliers, we reported the same coverage probability and average size as in Experiment 1. For outliers, we reported the detection accuracy. If we suppose there are s outliers, the formula of the detection accuracy is $|\{C(X_i) = \emptyset : X_i \text{ is an outlier}\}|/s$.

Table 2 demonstrates the outcomes of Experiment 2 on FCI. The coverage of inliers is not affected by the import of outliers. It still achieves 95% coverage as pre-specified. However, the size of predictive sets is influenced. The average is less than 1, which means the algorithm mistakenly classified some inliers as outliers. As for outliers, the model can distinguish at an accuracy of 0.7673 and 0.7465. Thus, the model can separate *Ankle boot* from others even it doesn't appear in training phase.

Contamination Rate	Inlier		Outlier Detection Accuracy
	Coverage	Size	
3%	0.9484	0.9611	0.7673
6%	0.9497	0.9535	0.7465

Table 2: **Results on Fashion-MNIST with outliers** We report the coverage and size for inliers and detection accuracy for outliers. Each result is the mean of 100 independent trials.

5 Discussion

In modern applications, the testing data has a distributional shift from training data or contains contamination that violates the exchangeable assumption for data-splitting conformal prediction. Our approach quantifies the uncertainty through the conditional adversarial flow, which is robust to the distributional change and outliers. Since we need to train a flow model for each class, the overall architecture is more complex than the classical classification model. As a future work, we aim to improve the network architecture, which combines all the mappings into a single process. Finally, our experimental results are limited to the fashion-MNIST data with only ten classes. We expect to extend our work to a wider variety of real-world problems with a large number of classes.

References

Anastasios Angelopoulos, Stephen Bates, Jitendra Malik, and Michael I Jordan. Uncertainty sets for image classifiers using conformal prediction. *arXiv preprint arXiv:2009.14193*, 2020.

Mihalj Bakator and Dragica Radosav. Deep learning and medical diagnosis: A review of literature. *Multimodal Technologies and Interaction*, 2(3):47, 2018.

Richard A Davis, Keh-Shin Lii, and Dimitris N Politis. Remarks on some nonparametric estimates of a density function. In *Selected Works of Murray Rosenblatt*, pages 95–100. Springer, 2011.

Vincent Dumoulin and Francesco Visin. A guide to convolution arithmetic for deep learning. *arXiv preprint arXiv:1603.07285*, 2016.

Isaac Gibbs and Emmanuel Candes. Adaptive conformal inference under distribution shift. *Advances in Neural Information Processing Systems*, 34, 2021.

Ian Goodfellow, Jean Pouget-Abadie, Mehdi Mirza, Bing Xu, David Warde-Farley, Sherjil Ozair, Aaron Courville, and Yoshua Bengio. Generative adversarial nets. In *Advances in Neural Information Processing Systems*, volume 27, 2014a.

Ian Goodfellow, Jean Pouget-Abadie, Mehdi Mirza, Bing Xu, David Warde-Farley, Sherjil Ozair, Aaron Courville, and Yoshua Bengio. Generative adversarial nets. *Advances in neural information processing systems*, 27, 2014b.

Arthur Gretton, Karsten M Borgwardt, Malte J Rasch, Bernhard Schölkopf, and Alexander Smola. A kernel two-sample test. *The Journal of Machine Learning Research*, 13(1):723–773, 2012.

Chuan Guo, Geoff Pleiss, Yu Sun, and Kilian Q Weinberger. On calibration of modern neural networks. In *International Conference on Machine Learning*, pages 1321–1330. PMLR, 2017.

Chirag Gupta, Arun K Kuchibhotla, and Aaditya Ramdas. Nested conformal prediction and quantile out-of-bag ensemble methods. *Pattern Recognition*, 127:108496, 2022.

Kaiming He, Xiangyu Zhang, Shaoqing Ren, and Jian Sun. Deep residual learning for image recognition. In *Proceedings of the IEEE conference on computer vision and pattern recognition*, pages 770–778, 2016.

Jing Lei and Larry Wasserman. Distribution-free prediction bands for non-parametric regression. *Journal of the Royal Statistical Society: Series B (Statistical Methodology)*, 76(1):71–96, 2014.

Qiao Liu, Jiaze Xu, Rui Jiang, and Wing Hung Wong. Density estimation using deep generative neural networks. *Proceedings of the National Academy of Sciences*, 118(15), 2021.

Xiao-Li Meng. Posterior predictive p -values. *The annals of statistics*, 22(3):1142–1160, 1994.

Radford M Neal. *Bayesian learning for neural networks*, volume 118. Springer Science & Business Media, 2012.

Jeremy Nixon, Michael W Dusenberry, Linchuan Zhang, Ghassen Jerfel, and Dustin Tran. Measuring calibration in deep learning. In *CVPR Workshops*, volume 2, 2019.

Harris Papadopoulos. *Inductive conformal prediction: Theory and application to neural networks*. INTECH Open Access Publisher Rijeka, 2008.

Harris Papadopoulos, Kostas Proedrou, Volodya Vovk, and Alex Gammerman. Inductive confidence machines for regression. In *European Conference on Machine Learning*, pages 345–356. Springer, 2002.

John Platt et al. Probabilistic outputs for support vector machines and comparisons to regularized likelihood methods. *Advances in large margin classifiers*, 10(3):61–74, 1999.

Qing Rao and Jelena Frtunikj. Deep learning for self-driving cars: Chances and challenges. In *Proceedings of the 1st International Workshop on Software Engineering for AI in Autonomous Systems*, pages 35–38, 2018.

Yaniv Romano, Matteo Sesia, and Emmanuel J. Candès. Classification with valid and adaptive coverage. In *Proceedings of the 34th International Conference on Neural Information Processing Systems*, NIPS’20, 2020.

Karen Simonyan and Andrew Zisserman. Very deep convolutional networks for large-scale image recognition. *arXiv preprint arXiv:1409.1556*, 2014.

Robert A Stine. Bootstrap prediction intervals for regression. *Journal of the American Statistical Association*, 80(392):1026–1031, 1985.

Vladimir Vovk. Conditional validity of inductive conformal predictors. In *Asian conference on machine learning*, pages 475–490. PMLR, 2012.

Vladimir Vovk, Alex Gammerman, and Glenn Shafer. *Algorithmic Learning in a Random World*. Springer, New York, 2005.

N. C. Weber. A martingale approach to central limit theorems for exchangeable random variables. *Journal of Applied Probability*, 17(3):662–673, 1980.

Xin Xing, Zuofeng Shang, Pang Du, Ping Ma, Wenzuan Zhong, and Jun S Liu. Minimax nonparametric two-sample test. *arXiv preprint arXiv:1911.02171*, 2019.

Jun-Yan Zhu, Taesung Park, Phillip Isola, and Alexei A. Efros. Unpaired image-to-image translation using cycle-consistent adversarial networks. In *2017 IEEE International Conference on Computer Vision (ICCV)*, pages 2242–2251, 2017.